

AD-A099 765

NAVAL RESEARCH LAB WASHINGTON DC

F/G 17/9

RESULTS OF A FEASIBILITY STUDY FOR DETERMINING THE YAW ANGLE OF—ETC(U)

MAY 81 F D QUEEN, J J ALTER

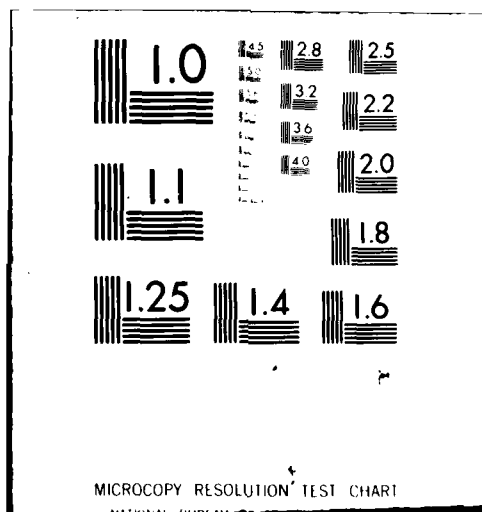
UNCLASSIFIED NRL-8480

NL

For I
AL-100



END
DATE
FILMED
6-81
DTIC



(12) LEVEL II

NRL Report 8480

**Results of a Feasibility Study for
Determining the Yaw Angle of a Landing Aircraft**

F. DONALD QUEEN AND JAMES J. ALTER

*Target Characteristics Branch
Radar Division*

May 27, 1981

**DTIC
ELECTE
JUN 5 1981
S D
B**



**NAVAL RESEARCH LABORATORY
Washington, D.C.**

Approved for public release; distribution unlimited.

81 6 05 011

AD A099765

DTIC FILE COPY

7

SECURITY CLASSIFICATION OF THIS PAGE (When Data Entered)

REPORT DOCUMENTATION PAGE		READ INSTRUCTIONS BEFORE COMPLETING FORM
1. REPORT NUMBER NRL Report 8480	2. GOVT ACCESSION NO. AD-A099765	3. RECIPIENT'S CATALOG NUMBER
4. TITLE (and Subtitle) RESULTS OF A FEASIBILITY STUDY FOR DETERMINING THE YAW ANGLE OF A LANDING AIRCRAFT	5. TYPE OF REPORT & PERIOD COVERED Final report, January 1976 to October 1979	6. PERFORMING ORG. REPORT NUMBER
7. AUTHOR(s) F. Donald Queen and James J. Alter	8. CONTRACT OR GRANT NUMBER(s)	
9. PERFORMING ORGANIZATION NAME AND ADDRESS Naval Research Laboratory Washington, DC 20375	10. PROGRAM ELEMENT, PROJECT, TASK AREA & WORK UNIT NUMBERS 62721N; XF2F; 232,061 53-0650-0-1	
11. CONTROLLING OFFICE NAME AND ADDRESS Naval Electronic Systems Command Washington, DC 20360	12. REPORT DATE May 27, 1981	13. NUMBER OF PAGES 19
14. MONITORING AGENCY NAME & ADDRESS (if different from Controlling Office)	15. SECURITY CLASS. (of this report) Unclassified	15a. DECLASSIFICATION/DOWNGRADING SCHEDULE
16. DISTRIBUTION STATEMENT (of this Report) Approved for public release; distribution unlimited.		
17. DISTRIBUTION STATEMENT (of the abstract entered in Block 20, if different from Report)		
18. SUPPLEMENTARY NOTES		
19. KEY WORDS (Continue on reverse side if necessary and identify by block number) Yaw angle Crab angle		
20. ABSTRACT (Continue on reverse side if necessary and identify by block number) A study was conducted to determine a means of measuring the yaw angle (crab angle) of an aircraft landing in zero-zero visibility conditions. The results of flight tests using the technique judged most promising are described. This technique used the characteristics of the radar returns obtained when the beam aspects of the aircraft were illuminated with a high-range-resolution radar. The range-time profiles of the sides of the aircraft were processed to determine the delay time between maximum correlation of the two waveforms. This delay is shown to be directly related to the crab angle. While success was achieved using manual data processing, automatic data processing did not produce consistent (Continued)		

DD FORM 1 JAN 73 1473

EDITION OF 1 NOV 65 IS OBSOLETE
S/N 0102-014-6601

SECURITY CLASSIFICATION OF THIS PAGE (When Data Entered)

20. ABSTRACT (Continued)

results when the aircraft geometry was complex. It was concluded that the profiles did not match because of differences in the radar characteristics. A radar technique employing switched RF oscillators is recommended for further testing.

CONTENTS

INTRODUCTON	1
THE AUTOMATIC LANDING SYSTEM	1
THE PROBLEM	1
MEASUREMENT ACCURACY	1
SELECTION OF SENSORS	1
REFERENCE MEASUREMENT	3
TEST RESULTS WITH ANALOG DATA	4
DATA COLLECTION SYSTEM	6
DATA PROCESSING RESULTS	6
PROPOSED X-BAND MEASUREMENT SYSTEM	14
CONCLUSIONS AND DISCUSSION	15
RECOMMENDATION	16
ACKNOWLEDGMENTS	16
REFERENCES	16

Accession For	
NTIS GRA&I	<input checked="checked" type="checkbox"/>
DTIC TAB	<input type="checkbox"/>
Unannounced	<input type="checkbox"/>
Justification	
By _____	
Distribution/	
Availability Codes	
Dist	Avail and/or Special
A	

RESULTS OF A FEASIBILITY STUDY FOR DETERMINING THE YAW ANGLE OF A LANDING AIRCRAFT

INTRODUCTION

The purpose of this project was to investigate methods of measuring the yaw angle (or crab angle) of an aircraft, using sensors which would operate in zero-visibility conditions. Yaw angle is the angle between the fore-aft axis of the aircraft and the aircraft velocity vector. The application of these sensors is to a ground-based automatic landing system which is intended for all-weather landing operations.

THE AUTOMATIC LANDING SYSTEM

The principal components of a ground-derived landing system are the surveillance radar and the precision approach radar (PAR). The surveillance radar detects the aircraft at ranges to 60 nmi for ordering the aircraft for approach. The precision approach radar acquires the aircraft at up to 10 nmi and measures the bearing, elevation, and range of the target. These measurements are used to control the position and velocity of the aircraft through a computer and an uplink to the aircraft flight-control system. Both the trim and the engine thrust are controlled through the uplink. The PAR measurements must be sufficiently accurate to land the aircraft within ± 4.6 m (± 15 ft) of the midpoint of an arresting cable and ± 12.2 m (± 40 ft) longitudinally from the extended cable. If there is no crosswind, the controls of the aircraft can be frozen at a fixed point before touchdown and the aircraft will land at a predictable point. When crosswinds exist and the aircraft is yawed (crabbed) to reach the projected touchdown point, the crab must be removed prior to touchdown.

THE PROBLEM

The effort was directed toward the investigation of sensors to measure the crab angle from 10 to 3 s before touchdown. A secondary objective was an altitude measurement for guidance in the flare or flare-out maneuver. Flare is a decrease in the rate of descent which may be 1.83 to 4.88 m/s (6 to 16 ft/s) along the glide path to 0.6 to 0.91 m/s (2 or 3 ft/s) at touchdown. Since carrier-based aircraft are not required to flare and the projected accuracy of the PAR for height measurement was sufficiently accurate for flare guidance when required, primary effort was directed at the crab-angle measurement.

MEASUREMENT ACCURACY

The accuracy goal for the crab-angle measurement was $\pm 1^\circ$. The accuracy was based on Military Specification MIL-A-8863A, which lists the mean value of the yaw angle as 0° and the standard deviation as 3° . While it is recognized that aircraft are tested at crab angles larger than 3° , the stress on the landing gear depends on a combination of factors such as the approach speed, sink rate, roll, pitch, and landing weight in addition to the crab angle. Simultaneous extremes in several of these values could cause failure of the landing gear.

SELECTION OF SENSORS

We approached the problem by examining potential sensors using electromagnetic waves, mechanical waves, etc. in various ground- and air-derived systems. Table 1 lists the variables in the aircraft

Table 1 — Components of Aircraft Attitude and Position Obtainable with Sensors Based on Observable Phenomena Listed

Observable Phenomena		Ground-Derived Components*		Air-Derived Components*	
		Air Unaided	Air Aided	Ground Unaided	Ground Aided
Magnetic	(Static)	4-5-6	1-4-5-6	1	1-3-5-6
Electric				2-3	2-3
Audio	(EM)	1-4-5-6	1-2-3-4-5-6	4	1-2-3-4-5-6
RF			5-6		1-5-6
μ wave			1-2-3-4-5-6		1-2-3-4-5-6
Gamma Rays		4-5-6	5-6	4	1-2-3-4-5-6
Acoustics			1-4-5-6		
Inertial				1-2-3	1-2-3

*1 = yaw; 2 = roll; 3 = pitch; 4 = height; 5 = lateral position; 6 = longitudinal position

attitude and position which could be accommodated by the sensors. Reference 1 describes an air-aided technique using audio-frequency electromagnetic waves, and Ref. 2 describes an air-derived system with ground aids. Since a requirement for a totally ground derived system was established, radar was given primary emphasis. Experiments were performed with a Doppler radar [3] and a high-range-resolution radar (HRRR) system based on a technique proposed by Sperry Univac. Both systems were used to view the beam and near-beam aspects of the aircraft as it passed the radar (Fig. 1). Since the crab angle must be known at least three seconds before touchdown, the radars were located on the ground in front of the runway. Aircraft passes were arranged to provide no crab (the aircraft fore-aft axis is parallel with the vector), right and left crab, and passes between the sensors with an angular offset from the runway centerline projection. While the angular offsets, which will be referred to as crosstrack, could be determined by processing the Doppler data, the crab angles could not be accurately determined. The HRRR technique did provide valid crab-angle results using manual processing of data from one radar; therefore, it was decided to pursue this technique using automatic data processing.

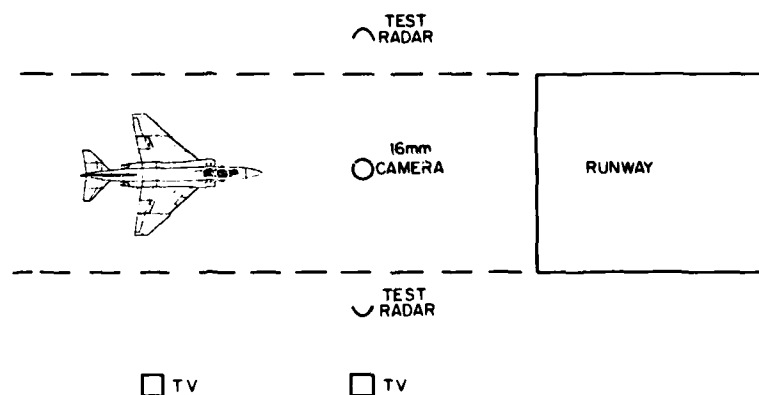


Fig 1 — Test configuration for determination of crab angle by radar and optical systems

REFERENCE MEASUREMENT

To evaluate the angle measurements obtained from sensors under test, a reference system was required. Both film and television were used. The cameras were boresighted to surveyed points and calibrated by photographing and recording a calibrated target placed at a distance of 15.2 m (50 ft). A 16-mm camera on the runway centerline pointed vertically was used as the reference for yaw angle. It was mounted to a plate which also contained a wire stretched across the lens at a distance of 1.2 m (4 ft). The wire was aligned with the runway centerline. The yaw angle is found by plotting two symmetrical points on the aircraft and measuring the angle between a line constructed between the two points and the centerline (Fig. 2). If the ground track of the aircraft is not down the centerline, the offset angle or crosstrack must be determined. This is done by constructing a line from the projected image of a distinct feature on the fuselage for successive film frames (Fig. 3). The angle between the constructed line and the centerline is the crosstrack angle. The actual angle of the aircraft with respect to the projected centerline of the runway is the combination of the yaw and crosstrack angles.

Fig. 2 — Measurement of crab angle from film reference system

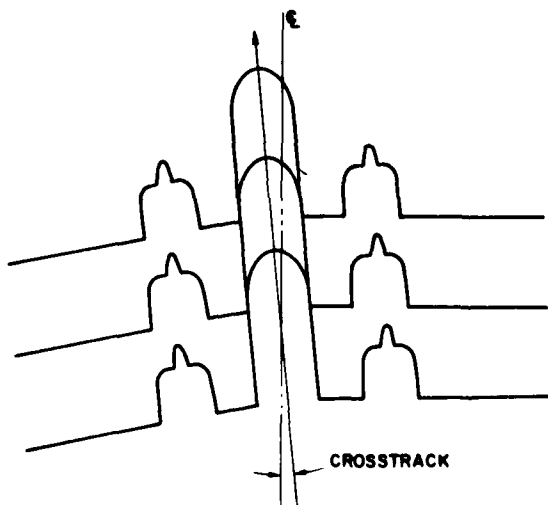
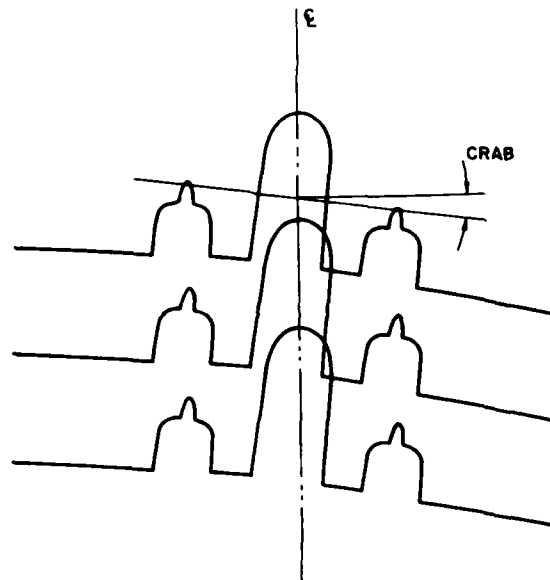


Fig. 3 — Determination of cross track from film reference system

A television system is used to determine aircraft velocity (Fig. 1). A time code accurate to 0.1 s is observed with a TV camera whose output is mixed with the outputs of the cameras placed along the runway projection. The video from the camera which the aircraft passes first is recorded on tape together with the time code. After the aircraft passes through the field of view of this camera, the video from the second camera is switched to the recorder. The time difference required for a fixed object on the aircraft to pass both cameras can be measured to within two TV fields, or 33 ms. Considering a nominal 100-knot velocity for the aircraft and a 42.7-m (140-ft) separation between cameras, the velocity can be determined to ± 2.13 m/s (± 7 ft/s). In the processing used to determine the crab angle from the system under test, this accuracy can result in a $\pm 0.2^\circ$ uncertainty in the angle.

TEST RESULTS WITH ANALOG DATA

Initially one radar was purchased to determine the repeatability of the range profile of an aircraft from pass to pass and also to examine the nature of the landing profile, i.e., the numbers of scatterers and their relative amplitudes. Photographs of an oscilloscope displaying amplitude vs range were used for data collection. The camera moved the film for physical separation of successive traces. The PRF of the radar was limited to 100 Hz so that signal amplitudes could be resolved. The sweep speed of the oscilloscope was set for 3.04-m (10-ft) range per centimeter. The center position of the trace was a reference for a target passing over the centerline at 15.2-m (50-ft) altitude. Figure 4 shows one data run on the S-2D. Successive traces separated by 0.01 s show that different distinct scatterers on the aircraft are observed with elapsed time. The reconstructed trace beneath the aircraft profile depicts the major reflecting surfaces on the aircraft. A more detailed analysis of the returns from the major reflectors is considered later. The vertical bars on the right of the film represent the BCD time code. Each change marks a 0.1-s interval corresponding to a time code on the TV monitor. This presentation allows location of the point in each data run when a reference point on the aircraft passes a line through the radar and TV camera locations.

The film strips from seventeen data runs of one flight were aligned with respect to a time (t_0) when the main wheels passed the radar. The run-to-run character of the received range vs time profiles were observed to be very similar. It was also observed that the displacement of the signature from time zero correlated with the crab angle. Figure 5 shows five runs selected to demonstrate this observation. The reference angle is the combination of the crab angle and the crosstrack angle. For example, when the crab is left and the aircraft is drifting right such that the ground track is not parallel to the runway centerline, the actual angle is the difference between the crab and the crosstrack. In the runs shown in Fig. 5, the radar is viewing the starboard side of the aircraft. For the first run with 6° left crab the radar reflections from the outboard wing station, the engine nacelle, and the fuselage occur before t_0 . When the crab angle is to the right, the returns occur after t_0 . This is because the surfaces are normal to the radar beam earlier in time when the nose of the aircraft is to the left than when the nose is to the right. For these data runs the corner formed by the wing station was large because of equipment installation on the wing station. It was observed that the return from the outboard nacelle peaked twice, as indicated with arrows on Fig. 4. The first peak was attributed to the portion parallel to the fore-aft axis of the aircraft. The second peak was always much larger in amplitude and could be caused by the after-section of the nacelle, which is about 5° from the fore-aft axis. The time between the 5° change ($t_2 - t_1$) and the time between the wheel crossing and the peak at 90° ($t_1 - t_0$) were used to determine the approximate crab angle from

$$\frac{t_2 - t_1}{5^\circ} = \frac{t_1 - t_0}{\text{crab angle}}$$

where t_0 = time wheels pass the center of the radar beam,

t_1 = time of peak parallel to fore-aft axis, and

t_2 = time of peak 5° from fore-aft axis.

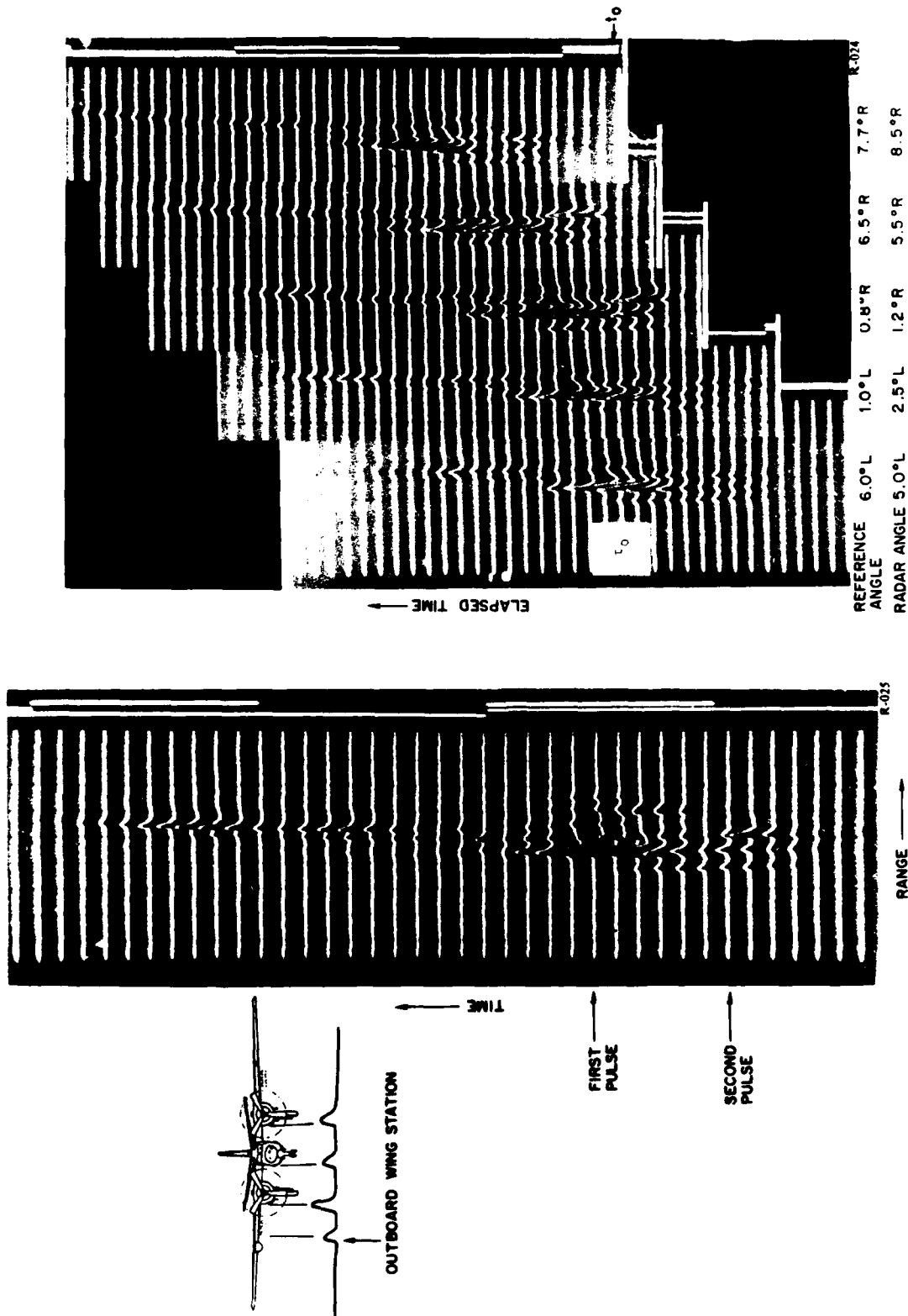


Fig. 5 — Oscilloscope photographs of five data runs using the S-2D aircraft with differing crab angles

Fig. 4 — Range profile of the S-2D

The results of the computations for the five data runs are shown on Fig. 5. The accuracy of the results is limited by the low PRF, because times can only be resolved to 0.01 s.

The fact that HRRR data could be used to extract crab angles indicated that further investigation was warranted. Since in zero visibility the time t_0 would be unknown, the use of two radars was considered to eliminate the requirement for t_0 . The theory of determining the angle can be explained with reference to Fig. 6, which shows an aircraft without crab passing between two radars. In position 1 a specular reflection would be seen by both radars from points near the nose normal to the beam. In position 2 the points would move around the curved surface until in position 3 the points normal to the radar beam are on the rear section of the fuselage. The returned signals would produce a range profile with elapsed time. If the aircraft has a left crab angle (Fig. 7), the points which produced simultaneous signal returns in position 1 when the aircraft had no crab will be shifted. The beam from radar 1 will be normal to this point before the beam from radar 2; therefore, the radar 2 profile will be delayed with respect to that from radar 1. The amount of delay should be a measure of the crab angle.

DATA COLLECTION SYSTEM

To provide a means for computer processing of data, digital recordings of range and amplitude were required. The data collection system is shown in the block diagram in Fig. 8. The transmitter generates a pulse of approximately 5 ns. A second independent transmitter is used for the opposite side of the runway. A 1-kHz repetition frequency generated by the master timing unit was used. The key pulse to the second transmitter was delayed by 1 μ s to avoid mutual interference between the two radars. Cables to the radars were matched in length so that delays would be uniform. After RF amplification and video detection and amplification the signal was split into independent range and amplitude measurement channels. For range the signal was compared to a fixed threshold set 3 dB above the receiver noise level. The comparator generated a video pulse which controlled the turn-off time of six counters. The clock frequency of the counters was 512 MHz, with each cycle representing 0.3 m (1 ft) in range. All counters were zeroed on the transmitter pulse and clocked when the transmitter actually fired. On the first received pulse the clock to counter A was inhibited, and a signal path to counter B was established. A second received pulse for the same transmitted pulse then gated off the clock to counter B and allowed counter C to be stopped on the third pulse. All counters stopped by received pulses from scatterers across the aircraft are stored for recording. Counters exceeding the maximum range are zeroed.

The amplitude of the signal for each range measurement was recorded to eight levels. Power dividers were used to split the signal for application to the inputs of seven comparators. The thresholds to the comparators were set by a precision voltage divider, with each voltage level twice the preceding lower level. The lowest threshold level was twice the level of the range comparator threshold, so that a range measurement could have a zero amplitude indicating the signal was 3 to 6 dB above noise. The eight-level data were converted to 3-bit words for recording.

DATA PROCESSING RESULTS

A plot of the range profile for a Piper Navaho is shown in Fig. 9. The recording process is initiated by the first detection in either radar. In this case radar 1, viewing the starboard side of the aircraft, detects the aircraft first. This indicates that the aircraft has left crab. The magnitude of the angle was found by delaying the profile of radar 1 until the best match with radar 2 was found. This procedure and the calculation of the angle is shown in Fig. 10. A cross-correlation routine was run in the computer on the 10 data runs of this flight. The angles calculated for nine of the ten data runs were within 0.3° of the reference angle. The remaining run had an error of 0.6°.

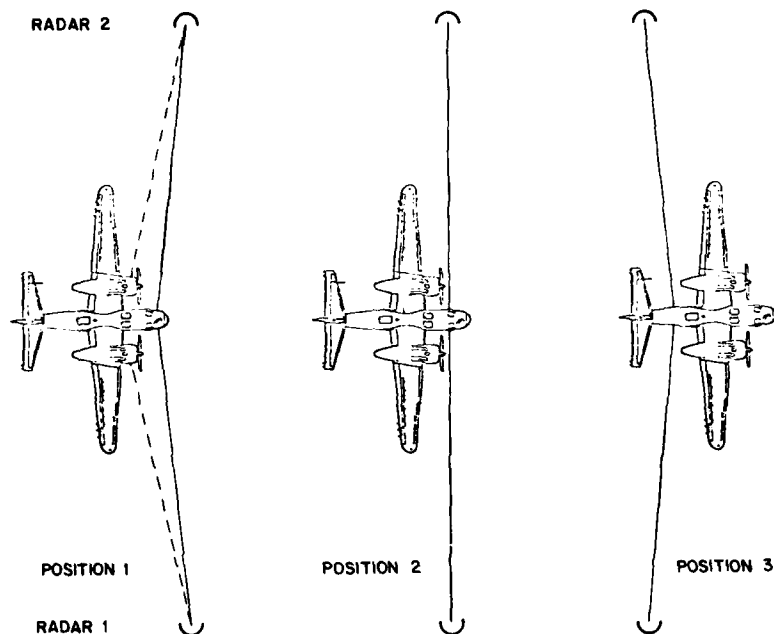


Fig. 6 — Change of flare point locations relative to the aircraft position. Dashed lines indicate additional points where an aircraft surface is normal to the beam.

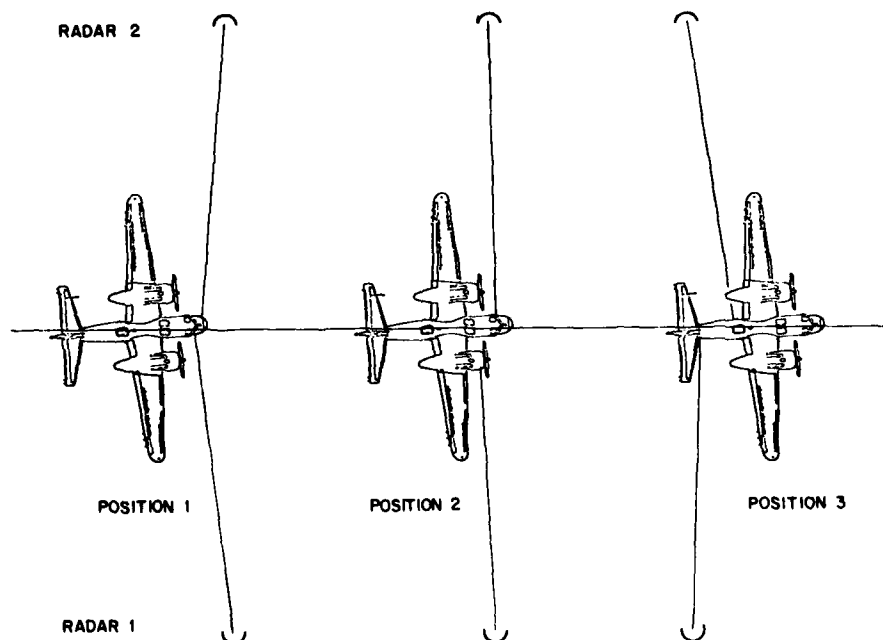


Fig. 7 — Flare points with left crab. Range-time profile for radar 1 leads that from radar 2.

QUEEN AND ALTER

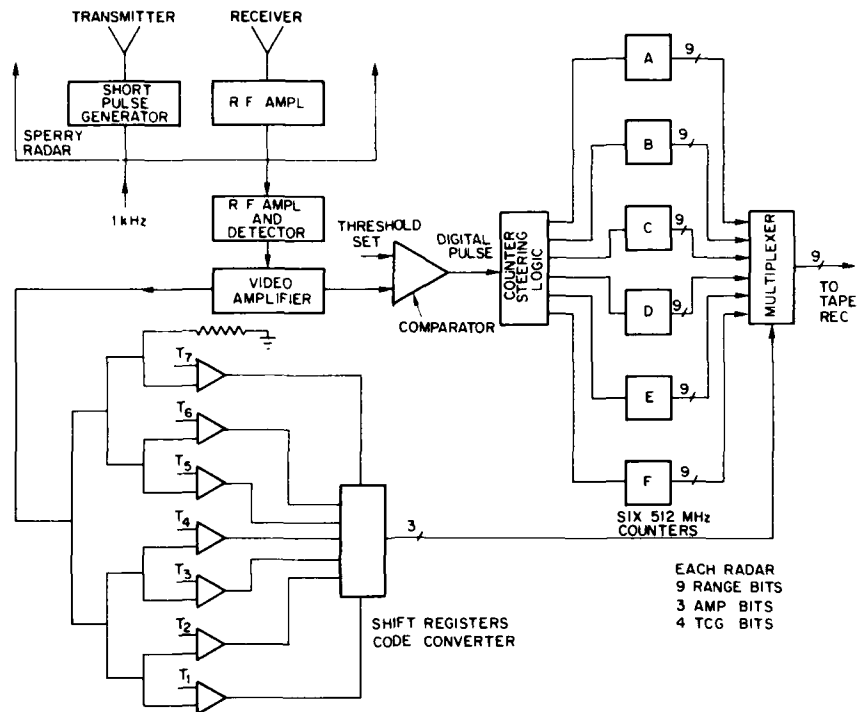


Fig. 8 — Data acquisition system for each radar

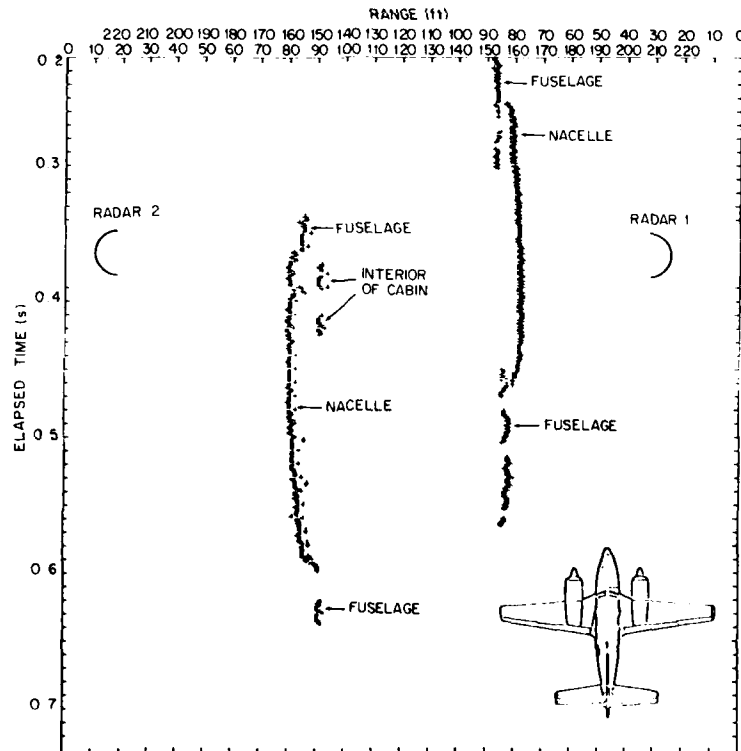


Fig. 9 — Range profile of the Piper Navaho. The aircraft had 'left crab' for this data run.

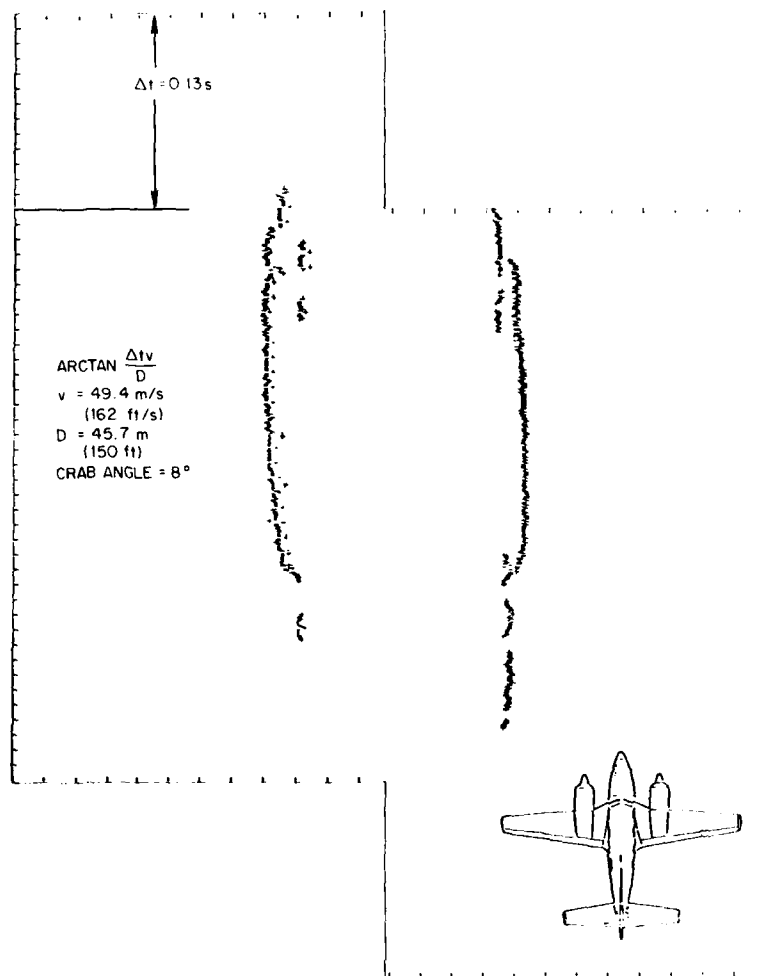


Fig. 10 — Profile of radar 1 delayed in time for best match with radar 2 profile

The cross-correlation processing first required modification of the range-time waveform to obtain a zero mean. The average range of the first detection from each radar for the 512 transmitted pulses was determined. When no return was observed in a pulse-repetition interval (PRI), that interval was not considered in the calculation of the average. The calculated mean values were subtracted from the first detections to produce a zero-mean set of samples which were placed in two 512 element arrays. Since some zero values were present, the array was arranged in the following manner:

$$R_{0i}(j) = \begin{cases} R_i(j) - m_i, & \text{if } R_i(j) \text{ is valid, for } i = 1 \text{ to } 2, j = 1 \text{ to } 512, \\ 0, & \text{if } R_i(j) \text{ is zero, i.e., no detection,} \end{cases}$$

where $R_1(j)$ and $R_2(j)$ represent the first detection on pulse j from radar 1 and radar 2, respectively, and $R_{01}(j)$ and $R_{02}(j)$ are the zero-mean arrays. The correlation coefficient for each shift, k , was calculated by

$$C_k = \sum_{j=1}^{512} \frac{R_{01}(j) \cdot R_{02}(j+k)}{\sigma_1 \sigma_2}, \quad -256 < k < 256,$$

where σ_1 and σ_2 are the standard deviations computed by

$$\sigma_i = \sum_{j=1}^{512} \sqrt{[R_{02}(j)]^2}, \quad i = 1, 2.$$

When $j + k$ was greater than 512 or less than 1, a value of zero was assumed for $R_{02}(j + k)$.

The shift which provided the largest correlation coefficient was used as the delay in radar pulses between the match of the profiles. The actual time is the number of shifts multiplied by the PRI of 1 ms.

Figure 11 shows the method used for computation of the crab angle from the time difference. In the time interval Δt , an aircraft with velocity v covers a distance $v\Delta t$. The angles θ_1 and θ_2 are equal, so that the distance $v\Delta t$ is divided equally about the line between the radars. The angle θ_1 is then

$$\theta_1 = \tan^{-1} \frac{v\Delta t}{D},$$

and the crab angle θ is equal to θ_1 . Over a reasonable limit of distances of offset from the centerline, this computation should provide the angle. The major problem is, of course, that if the aircraft is too far to one side of the runway the profiles would not match. This is because the aircraft would be in the beam of the nearer radar for a much shorter time.

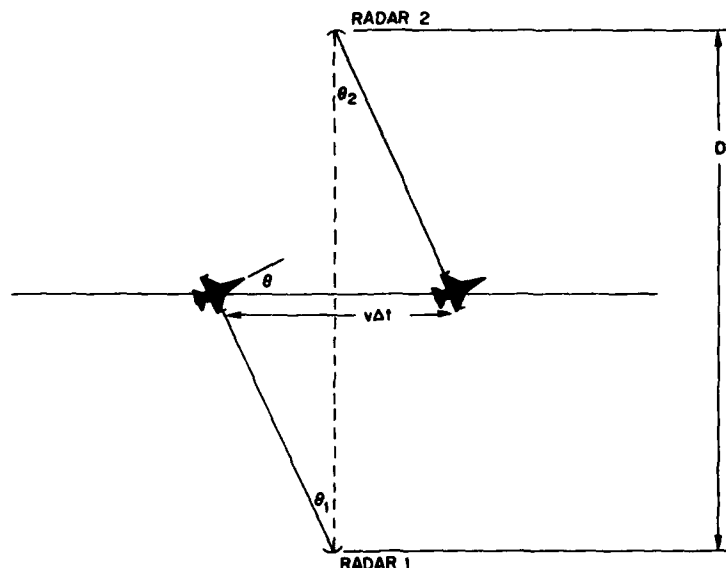


Fig. 11 — Development of crab angle measurement using the time difference between profile matches

The profile of the Navaho is rather simple, with the engine nacelles being the dominant scatterers. Since the technique would also be required to work with more complex targets, four flights were made using the S-2D. The data from the first two flight were not usable, due to a faulty connector in one case and interference from a system operating in the frequency range in the second case. The data from the third flight produced poor results using the cross-correlation technique. Several examples of the data acquired are shown in Figs. 12a and 12b. The reason that the cross-correlation results were poor is obvious in these data, because the profiles do not match. The data were examined to find which scatterers were detected by each radar. Since the radars were matched in antenna characteristics and in response on a standard target (sphere), several possibilities existed. Some of these possibilities are: (a)

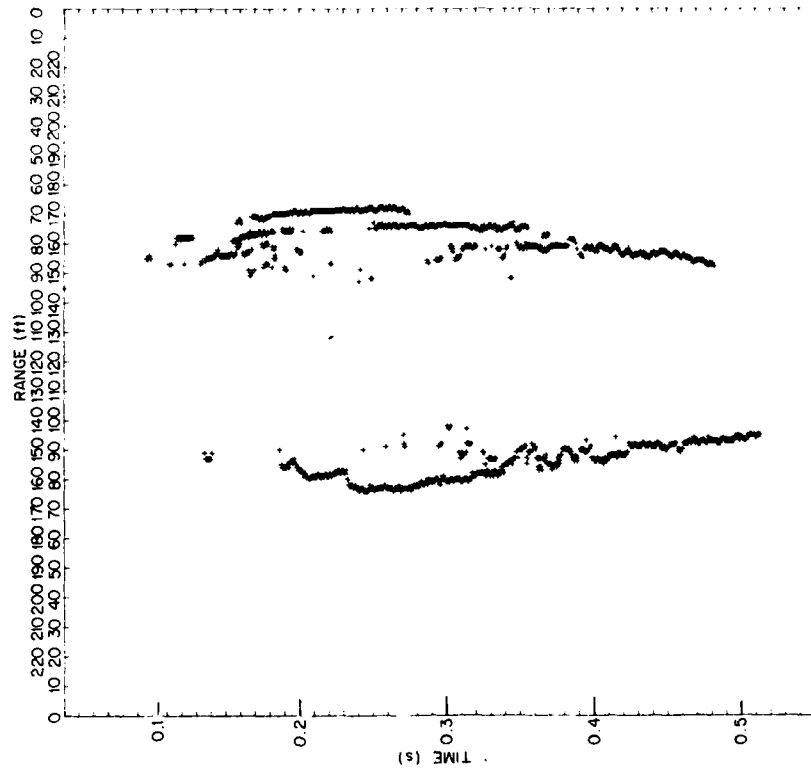


Fig. 12a — Profiles of the S-2D with no crab angle

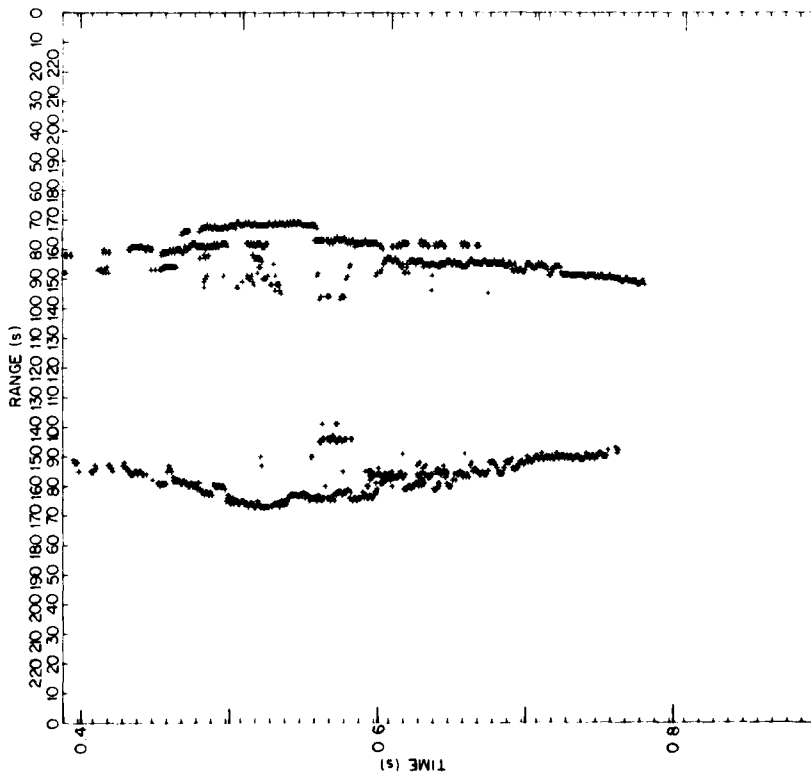


Fig. 12b — Profiles of the S-2D with 2.0° left crab angle

QUEEN AND ALTER

the aircraft is not symmetrical, (b) the viewing angles are different, (c) multipath conditions are not the same for the two radars, (d) the pulse widths (bandwidths) of the systems are not the same, and (e) the RF frequencies are sufficiently different to affect the radar cross section when several individual scatterers are in a range-resolution cell.

The S-2D was examined externally for structural differences between the port and starboard sides and none were found. One factor which cannot be accounted for is the internal position of the aircraft's radar antenna and its supporting structure, which may be seen by the measurement radar through the radome in the bottom of the fuselage.

Analysis of the range data indicates that the major scatterers are the engine nacelles (covers), the fuselage, and the outboard wing stations. The corner between the horizontal stabilizer and the fuselage is observed near the beam aspect. There are contributions from either the inboard section of the wheel covers or the propeller blade when it is normal to the radar beam and time-synchronized with the transmitted pulse. In Fig. 13 a typical range-time profile is shown with the scatterers identified. The major problem with these data is the lack of range resolution. The return in radar 1 from the nacelle at 0.86 to 0.87 and 0.94 to 0.95 on the time scale is seen because the amplitude of the signal is much higher than the return from the outboard wing station. The signal returned from the wing station is of higher amplitude between 0.87 and 0.94 and blocks the nacelle return. In this case, the detector capacitance is charged by a high voltage and the pulse is stretched into the following low-amplitude pulse, causing loss of the range information.

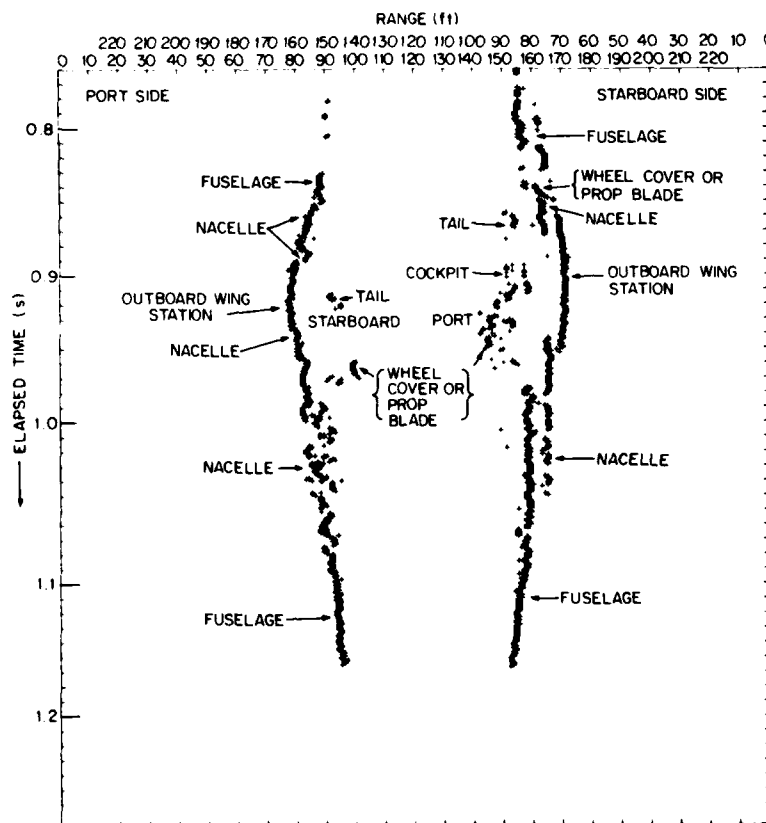


Fig. 13 — Profiles of the S-2D. Range values are measured in the slant plane and are not corrected for target travel. Crab angle is 1.1° left.

There is also physical blockage of major scatterers depending on the elevation aspect angle, which may not be the same for both radars if the aircraft has roll or is not on the runway centerline. To determine if the profile obtained with individual radars changed significantly with elevation angle, a flight was taken with aircraft altitudes varying from 15.2 to 36.6 m (50 to 120 ft). The cross-correlation coefficients were determined from radar 1 data on a run-to-run basis. Without correcting for aircraft velocity variations and range, which alter the duration of the range-time waveform, coefficients over 0.75 were obtained when a pass at 15.2 m (50 ft) was compared with passes up to 24.4 m (80 ft) in altitude. Above 27.4 m (90 ft) altitude the correlation coefficient dropped below 0.5. While part of the problem of low coefficients can be attributed to the range and velocity variations, another reason for the low value of the coefficient can be explained by observing the differences in profiles which would exist for altitudes of 15.2 and 27.4 m (50 and 90 ft) (Fig. 14). At 15.2 m (50 ft) the range difference between the wing station and nacelle is 1.22 m (4 ft). With the increase in altitude to 27.4 m (90 ft), the range difference drops to 0.6 m (2 ft) and the targets cannot be resolved by the system. For the radar separation used in the tests, which was necessary to maintain an adequate signal-to-noise ratio, the elevation angle difference is 15° between 15.2 and 27.4 m (50 and 90 ft). In the intended application the difference in the angles would not approach 15° . An offset from the centerline of 4.6 m (15 ft) would only produce a 10° difference, and pilots probably would not accept a roll angle of over 3° in zero visibility [4]. The 10° difference for offset can be reduced by placing the radars further apart.

During this same flight, radar 2 was moved to a side-by-side position with radar 1. As seen in Fig. 15, there is little similarity in the profiles. The fact that the duration of the signal from radar 2 is

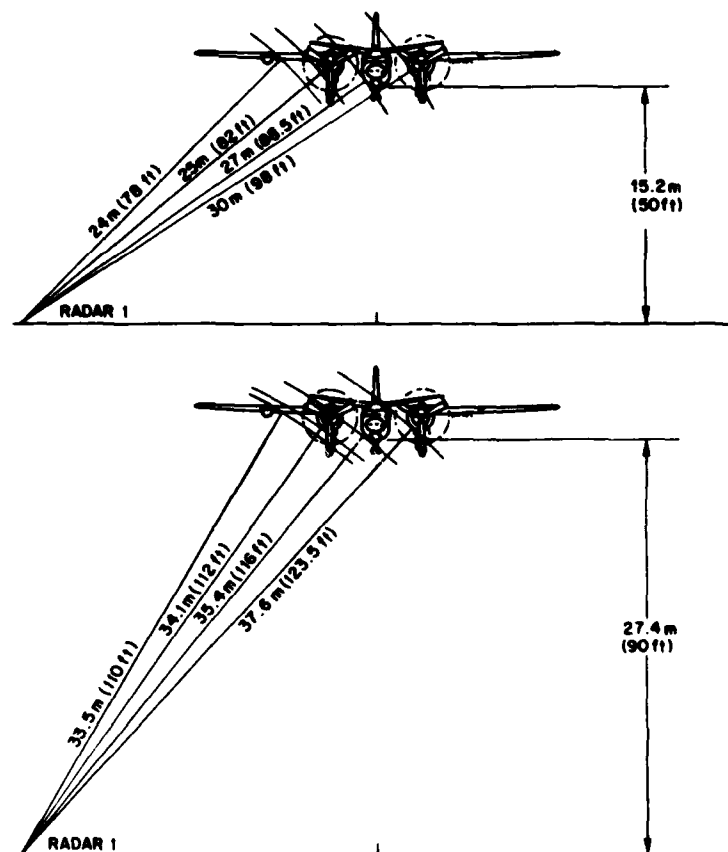


Fig. 14 — Plots showing decrease in range separation of reflectors on the S-2D as height increases

QUEEN AND ALTER

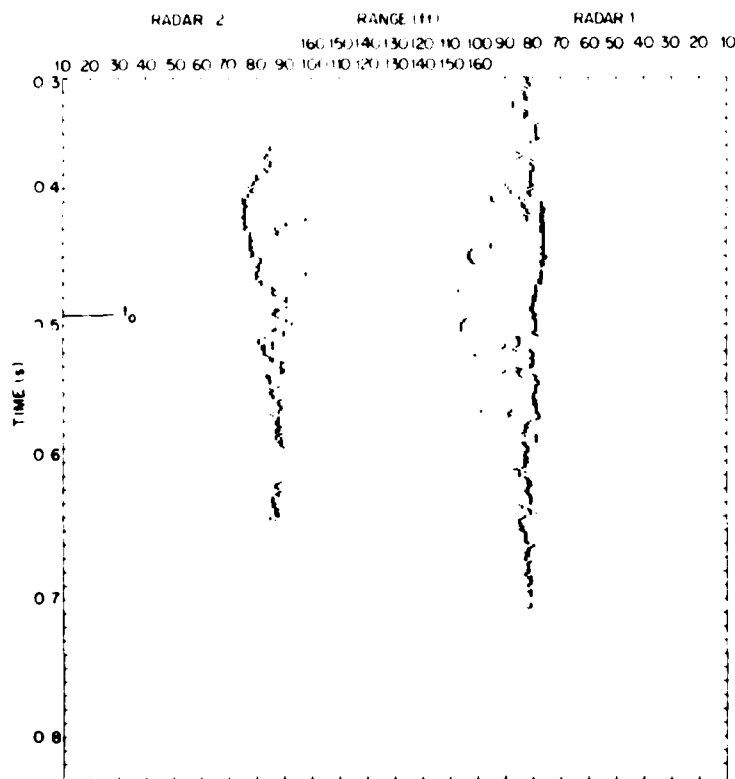


Fig. 15 — Profiles of the S-2D with the radars side by side, elevated to 35°. The aircraft altitude is 18.3 m (60 ft). Values are corrected to remove range change due to travel.

much shorter than that from radar 1 would indicate that the transmitted power or the sensitivity of radar 2 had changed during the flight. This is assumed because the azimuth beamwidths were found to be nearly identical in previous calibrations. Unfortunately, there is no way to monitor the transmitted power in the baseband radar design.

In all the data runs taken on the S-2D there is one consistent difference between the two profiles. The wing station is a dominant reflector at aspects just prior to the beam aspect as observed by one radar. A return from the wing station is seen at times by the second radar, but the nacelle is the more dominant reflector.

During an early flight with the Navaho one radar was used to measure altitude of the aircraft. The radar was positioned on the centerline and pointed vertically so that the aircraft would pass through the elevation axis of the antennas. One scatterer was observed and the average range (the accuracy of the digital system is ± 0.3 m or ± 1 ft) was in agreement with the optical measurement of the height of the bottom of the fuselage.

PROPOSED X-BAND MEASUREMENT SYSTEM

A system has been proposed which will eliminate any variability in the match of the radars. In this system a single CW source provides the RF frequency for both radars. During test flights the use of separate crystal-controlled sources was also planned.

The block diagram of the system is shown in Fig. 16. X-band operation was chosen because of the small component size. There would also be a reduction in the time the return from a scatterer would persist, because the lobing pattern is sharper as frequency is increased. This, in theory, could improve the range-time profile.

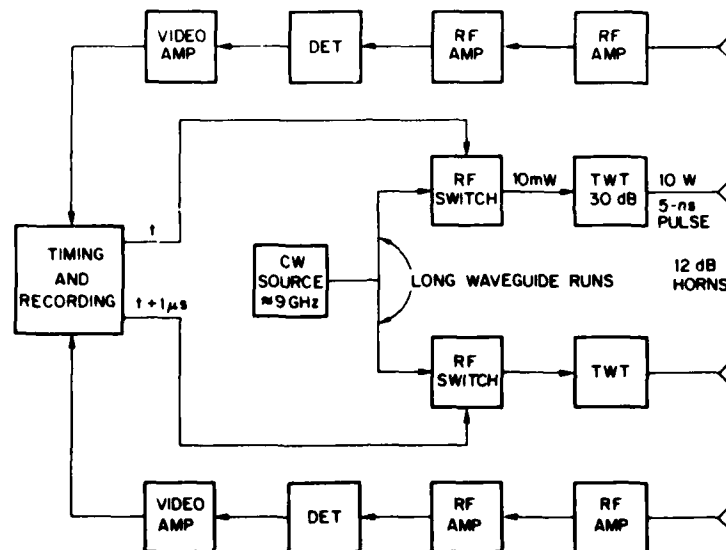


Fig. 16 — Proposed X-band measurement system

The major advantages of this system over the ones used are that the power level and frequency spectrum can be monitored within the system, the frequencies are matched, the horn characteristics are predictable, and more receiver dynamic range was designed into the system.

CONCLUSIONS AND DISCUSSION

The feasibility of range profiling of an aircraft to determine the yaw angle has not been resolved. The data collected are not of sufficient quality to allow a final conclusion to be drawn.

With the radars available for the measurements the profiles are dissimilar even when the radars are side by side, viewing the same aspects of the aircraft. The most likely source of the observed mismatches is a difference in the transmitted frequency spectra of the two radars. The returned signal from any objects on the aircraft in a range-resolution cell will be different under the assumed conditions, because the RCS varies with frequency. The phase difference between surfaces can result in a maximum signal or a null or any signal in between, depending upon the spacing of the surfaces and the wavelength.

Since multipath effects are unlikely to be the source of the problem, because the antenna characteristics are known to be the same, differences in transmitted spectra seem to be the most likely cause of the mismatches.

The X-band system proposed for final evaluation of the technique would have removed many problems which were encountered during the project. The transmitted frequency and power level in this system could be monitored without external antennas or calibrating targets. At the airfield it was difficult to assess the performance of standard targets near ground level with the system used because of multipath-induced signal-level variations.

Cross-correlation of the profiles obtained from run to run using one radar indicates that the profiling technique has potential. With the geometry used, that is, 45.7-m (150-ft) spacing between the radars, the elevation aspect changes rapidly with altitude. For improved profile match the separation of the radars could be increased to reduce the elevation aspect separation caused by offset from the centerline. Height determination using the radars viewing the sides of the aircraft is not practical unless the locations of the reflection points are resolved. The HRRR could be used for height measurement if located on the centerline and pointed to zenith. The fuselage is the lowest point on any aircraft and would be the dominant scatterer. Measurements of altitude during one flight with the Navaho demonstrated this technique to be useful.

The technique for crab-angle determination considered here is based on the aircraft reflectivity characteristics. If the wing stations of the aircraft are asymmetrically loaded, the profiles are likely to be different. Since the condition would be known to the pilot, special processing of the profile data could be employed to eliminate returns from the asymmetrical component. This would not be possible, however, if the individual scatterers could not be resolved.

Processing time is also a consideration in the technique employed. The cross-correlation processing requires 3 s in a high-speed computer. In 3 s an F-4 would travel about 230 m (750 ft). It is obvious that the processing time would have to be reduced to under one second. With special purpose hardware, a form of cross-correlation can be realized within this time frame.

Operational installation of this technique would require emplacement of a measurement system at several different locations prior to the end of the runway surface. The distance from the end of the runway for the first system could be as great as 300 or 600 m (1000 or 2000 ft). Obviously, it would be preferable if a technique could be devised which would require installation of equipment at only one location.

Finally, the range-profiling technique using the existing radars would work if a metal plate was installed near the wing tip. A two-sided corner reflector would be formed which would be insensitive to frequency and elevation aspect angle differences which are likely to exist. If aligned with the fore-aft axis of the fuselage, the returns would peak in amplitude when normal to the radar beam. The time difference between the peaks from the two radars would provide the crab angle.

RECOMMENDATION

If a requirement for zero-zero landing capability is established and the measurement system must be ground derived, the approach described herein should be investigated further.

ACKNOWLEDGMENTS

The assistance of B.L. Lewis in the development of the program is acknowledged. The many contributions of A.E. March, J.A. Alexander, H.H. Faust, P. Minthorn, and D.C. Hut are gratefully acknowledged.

REFERENCES

1. U.S. Patent 4,194,244, "Angle Sensing System," B.L. Lewis, March 18, 1980.
2. U.S. Patent 4,101,893, "Aircraft Landing Aid for Zero-Zero Visibility Landings," B.L. Lewis, July 18, 1980.
3. U.S. Patent 4,167,735, "Aircraft Orientation Determining Means," B.L. Lewis, September 11, 1979.
4. M. Kayton and W.E. Fried, *Avionics Navigation Systems*, John Wiley and Sons, New York, 1969.

DATE
ILME